

First spectral measurement of deuterium-tritium fusion γ rays in inertial fusion experiments

C. J. Horsfield and M. S. Rubery

*Atomic Weapons Establishment, Aldermaston, Reading, Berkshire RG7 4PR, United Kingdom*J. M. Mack, H. W. Herrmann, Y. Kim,* C. S. Young, S. E. Caldwell, S. C. Evans, T. S. Sedillo, A. M. McEvoy, N. M. Hoffman, M. A. Huff, J. R. Langenbrunner, G. M. Hale, and D. C. Wilson
Los Alamos National Laboratory, Los Alamos, New Mexico 87545, USA


W. Stoeffl, J. A. Church, and E. M. Grafil

Lawrence Livermore National Laboratory, Livermore, California 94550, USA

E. K. Miller

Mission Support and Test Services, Santa Barbara, California 93117, USA

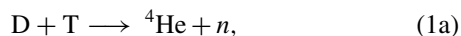
V. Yu Glebov

Laboratory for Laser Energetics, University of Rochester, Rochester, New York 14623, USA (Received 10 August 2017; revised 23 March 2021; accepted 23 July 2021; published 13 August 2021)

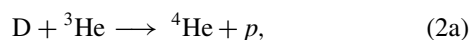
The R -matrix analysis of $A = 5$ nuclear systems has been partially validated by applying the technique to the ${}^5\text{Li}$ system and comparing the predicted γ -ray spectrum with historical data. R -matrix analysis of the similar ${}^5\text{He}$ system was then used to predict the γ -ray spectral shape for the deuterium-tritium (DT) reaction. The resulting spectra have been used in the analysis of DT implosions on the Omega laser where the γ -ray interaction rate was measured by a gas Cherenkov detector. Comparison of predictions to experiment confirmed the presence of both 16.75 and ≈ 13 MeV γ -ray contributions; analysis, using R -matrix spectra, yielded a ratio of γ -ray emission from a transition to the intermediate excited state to that from a transition to the ground state of $(2.1 \pm 0.4) : 1$, substantiating the first spectral measurement of the DT fusion γ ray in an inertial fusion environment.

DOI: [10.1103/PhysRevC.104.024610](https://doi.org/10.1103/PhysRevC.104.024610)**I. INTRODUCTION**

Fusion of deuterium (D, ${}^2\text{H}$) and tritium (T, ${}^3\text{H}$) nuclei produces an alpha particle and a 14.1 MeV neutron with a branching ratio of approximately 1. However, there exists another much less probable decay branch in which an intermediate excited state ${}^5\text{He}$ resonance emits a characteristic γ -ray spectrum according to



Gamma rays can be emitted as the resonance decays to the ground state (1b), alternatively a transition to an intermediate excited state (1c) can produce a lower energy γ ray. The energy spectrum of the emitted γ ray is expected to be similar to that obtained in the mirror nuclear $\text{D}{}^3\text{He}$ reaction:



which has been observed in accelerator experiments [1,2]. The $\text{D}{}^3\text{He}$ γ -ray spectrum consists of a peak at 16.66 MeV of width ≈ 1.2 MeV full-width-half-maximum (FWHM), corresponding to a direct transition from the 16.66 MeV excited state of ${}^5\text{Li}$ to its ground state. A broader peak is also observed near 12 MeV (FWHM = 3.5 MeV), corresponding to a transition from 16.66 MeV to an intermediate excited state at ≈ 4.5 MeV.

The DT gamma spectrum, as the mirror system to $\text{D}{}^3\text{He}$, is expected to exhibit similar properties (see Fig. 1). While accelerator-based measurements have successfully measured the γ_0 (i.e., the γ ray due to the transition to the ground state), analysis of the γ_1 (i.e., the lower-energy γ ray due to the transition to the intermediate excited state) is complicated by background from 14.1 MeV neutrons and neutron-induced γ rays [3–5]. Using inertial confinement fusion (ICF) implosions, new measurements mitigate this background issue and allow a more precise determination of the DT γ -ray spectral features. Gamma ray diagnostics, being developed for the National Ignition Facility (NIF) [6], require a thorough understanding of the DT spectrum in order to assess capsule performance [7–9]. We report the first experimental verification of the DT γ -ray spectrum in ICF experiments, including the presence of an intermediate excited-state transition.

* yhkim@lanl.gov

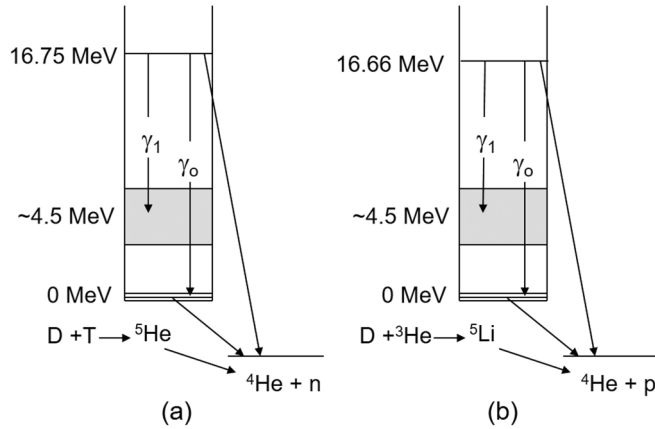


FIG. 1. Energy-level diagram for (a) ${}^5\text{He}$ DT reaction and (b) ${}^5\text{Li}$ D^3He reaction systems. Apart for some small variations in energy levels due to the differences in electric charge the energy-level diagrams are identical.

An R -matrix analysis [10] of reactions in the ${}^5\text{He}$ system predicts the spectral features of the DT γ -ray spectrum. This analysis determines, primarily on the basis of $n + {}^4\text{He}$ scattering data, the existence and shape of two spectral components, but not their relative intensities, $\Gamma_1 : \Gamma_0$, which was assumed, for a reasonable starting position, to set to a ratio of 1 : 1, as shown in Fig. 2 [11]. The properties of the ground- and intermediate-excited states of ${}^5\text{He}$ given in Ref. [12] were based on the R -matrix analysis from which the two spectral components shown in Fig. 2 are derived.

To validate the R -matrix technique, we considered the mirror D^3He reaction. An analogous analysis was performed on proton-alpha scattering data to predict the D^3He γ -ray spectrum, which was validated against past experiments [1]. When compared with the proton-alpha scattering data, the prediction shows excellent shape agreement, as shown in Fig. 3. In this figure the prediction was smoothed by a 1.28 MeV kernel to take account of the reported detector broadening [13]. The

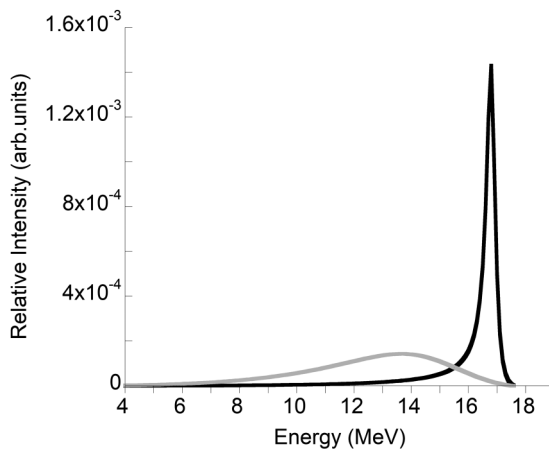


FIG. 2. Predicted spectral components of the DT fusion spectrum. Transitions to ground, γ_0 (black line), and intermediate-excited state, γ_1 (gray line), as generated by R -matrix analysis of n - α scattering experiments [1].

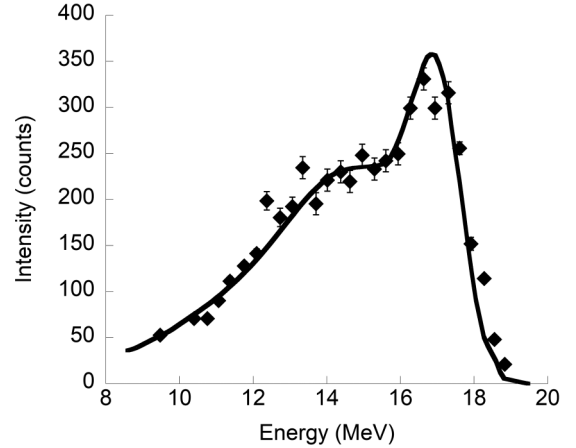


FIG. 3. Comparison between D^3He data (\blacklozenge) [1] and R -matrix prediction. The continuous line is the R -matrix prediction smoothed with a 1.28 MeV kernel; the discrete points are from Ref. [1]. $\Gamma_1 : \Gamma_0 = 1.4 : 1$ was used to match the simulation and data.

value of $\Gamma_1/\Gamma_0 = 1.4$ differs from the average values reported in Ref. [1] ($\Gamma_1/\Gamma_0 = 1.8$) but is within the value calculated with errors. This difference may also be due to the fact that Gaussian and Lorentzian fits were used in Ref. [1], weighting the ratio in favor of Γ_1 , while this paper uses a more realistic asymmetric profile associated with three-body decays.

II. EXPERIMENTAL APPROACH

To independently test the prediction for the DT γ -ray spectrum, ICF experiments [14] were performed using the Omega laser [15], which produced <200 ps FWHM DT fusion source. Difference in time-of-flight between fusion γ rays and neutrons allow for their temporal segregation at modest distances from the source, substantially avoiding the neutron-induced backgrounds, as compared with those observed in accelerator experiments. The desired γ -ray signals were observed with a gas Cherenkov detector (GCD) [16] (Fig. 4) with a response time of 7 ps when the energy threshold is set at 12 MeV and variable energy thresholding capability to further reduce undesirable radiation backgrounds.

Fusion γ rays impinging on the GCD converter produce relativistic electrons and positrons by pair production and Compton scattering. The electrons then enter a carbon-dioxide (CO_2) gas reservoir approximately 1 m in length where, if their speed exceeds the local speed of light, Cherenkov radiation is produced. The Cherenkov light is collected by Cassegrainian optics and focused onto a fast (80 ps) microchannel-plate photomultiplier tube (PMT), (PMT110,

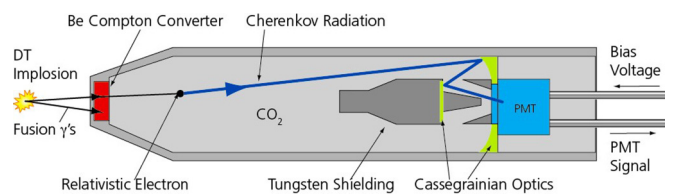


FIG. 4. Schematic of gas Cherenkov detector (GCD).

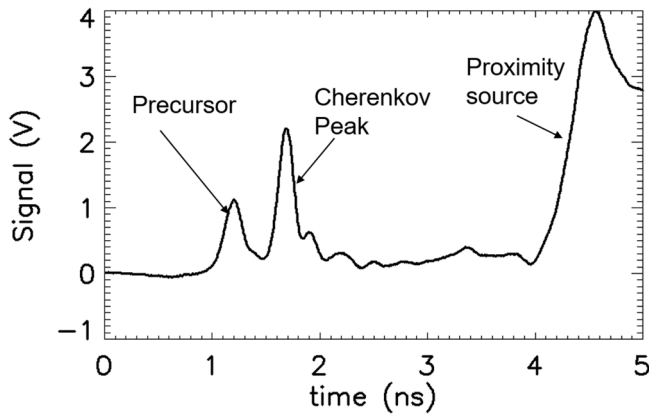


FIG. 5. Data from a DT fusion implosion Omega shot 61416, Cherenkov-energy threshold was 12 MeV.

Photek Ltd, UK) [17]. Tungsten shielding in front of the optics serve to protect the PMT from direct illumination from the fusion source.

For these experiments, the PMT was coupled to a 5 GHz traveling wave oscilloscope (Tektronix SCD5000) by a high bandwidth (4 GHz, bandwidth defined at the 3-dB roll-off point) cable (40 ft of 3/8 inch foam-flex, Andrews Corp.). The combined bandwidth of the entire system was 2.4 GHz, which equates to a temporal system response of 135 ps FWHM. The GCD Cherenkov-energy-production threshold is varied by changing the refractive index of the gas by altering the CO₂ pressure [18]. The targets used were CH shells of approximately 1 mm diameter, between 14 to 20 μ m wall thicknesses and filled with between 10 and 19 atmospheres of equimolar DT fuel. The targets were imploded with 27 kJ of 351 nm laser light using all 60 Omega beams. These targets produced fusion yields between 3×10^{12} and 3×10^{13} total neutron output and ion temperatures between 3.5 and 5.5 keV. An example of the data taken at a 12 MeV Cherenkov threshold is shown in Fig. 5.

III. DATA ANALYSIS

To compare with the predicted γ -ray spectrum to observation, we have adopted and developed a technique described previously [19] in which the spectrum is forward folded with *a priori* instrument response curves to create detector-responses as a function of threshold energy. The resulting threshold-energy-dependent responses were then integrated to generate predicted intensities that were compared with GCD measurements.

The previous work [19] to discern DT gamma transitions at 16.75 and 12–13 MeV, using ICF implosions, were inconclusive and improvements to the GCD and its operation have since been implemented; also, PMT gain calibration errors have been reduced significantly by operating the PMT at a single bias voltage. Signal levels were controlled with calibrated high-bandwidth electrical attenuators. The full *R*-matrix spectrum has been incorporated into the current analysis rather than assuming monoenergetic lines at two energies. Improved detector response models have been incorporated into

GEANT4 [20] and ITS-ACCEPT [21] Monte Carlo simulations. These codes have been extensively improved and benchmarked against dedicated experiments with γ -ray sources and electron-beam accelerator results [22]. Both the electron and γ -ray experiments have shown that the response shapes as a function of gamma energy and Cherenkov threshold were predicted within 5% when systematic uncertainties were removed from the absolute response.

Complete system characterization was not possible as some parameters remained prohibitively expensive to determine precisely, e.g., mirror reflectance and window transparency at wavelengths in the near UV and visible spectrum, PMT gain, photocathode performance, and possible tube degradation between characterization and actual measurement. These factors may be responsible for the overall disagreement in the benchmarking exercise. Ideally each would be calibrated separately.

Time resolved measurements were made of DT fusion sources at seven different Cherenkov energy thresholds between 6.3 and 14 MeV. The former threshold represents the maximum operating pressure of the GCD and the latter 14 MeV threshold corresponds to the sensitivity limit for the gamma yields considered in this work. These data were processed to remove the precursor peak shown in Fig. 5, which is inherently caused by γ rays striking the GCD detector wall and scattering directly into the PMT, bypassing the two-reflection optical path taken by the Cherenkov light. As a result, the precursor peak arrives earlier than the fusion gamma signal by 511 ps. Other potential (*n, n'* γ) proximity sources were eliminated by ensuring other diagnostics were at distances >7 cm from the target chamber center (TCC). A time-of-flight calculation for fusion neutrons to the proximity source and subsequent γ -rays to the GCD PMT ensured that any secondary gamma sources arrived >1 ns after the fusion gamma signal (<200 ps FWHM). The intensity in the Cherenkov peak was then determined by integration over time.

Energy-dependent detector responses were calculated at each threshold for which data were obtained. These responses were forward folded with computed spectra generated from varying combinations of the ground- and excited-state spectra, as shown in Fig. 2. The resulting intensity vs energy plots were then integrated over energy to provide a predicted intensity for comparison to experiment. Experimental data and theoretical predictions were normalized to the result at the 14 MeV threshold. This makes the analysis sensitive to the shape of the data set, but relatively insensitive to absolute intensity values. Also, this normalization removes the absolute-value sensitivity to the other systematic errors, mentioned above in the review of the benchmarking exercise [22], provided they do not change over the course of the experiment.

A comparison of the predicted responses between a spectrum consisting of the ground state only and a spectrum consisting of the summation of the ground and intermediate excited states with a ratio of $\Gamma_1/\Gamma_0 = 1$ is shown in Fig. 6. Both curves rise as the threshold energy decreases for two reasons:

- (1) The sensitivity of the diagnostic to a γ ray of a given energy increases as the threshold is lowered.

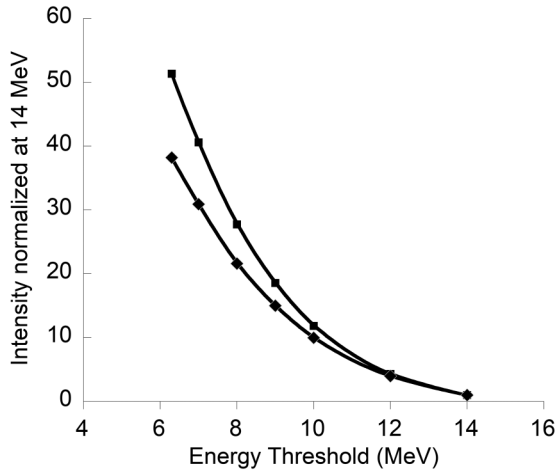


FIG. 6. Comparison of predicted intensity responses for ground state only (\blacklozenge) and combined spectrum of $\Gamma_1/\Gamma_0 = 1$ (\blacksquare). Normalized to result at 14 MeV threshold. The lines are third-order polynomial fits to guide the eye.

- (2) A lower threshold enables lower-energy γ rays to contribute to the intensity.

Experimental data plotted in Fig. 7 exhibit a similar trend, but with a much steeper curvature than the combined prediction. This indicates that the contribution from lower-energy γ rays is present and at a greater intensity than that shown in Fig. 2. This result establishes the existence and influence of transition to an intermediate excited state. Increasing the excited-state intensity achieves a closer fit to the experiment when a ratio of excited-state to ground-state spectra is adjusted to 2.1 : 1. The errors in these data are due to a combination of statistical spreading over several shots and integration errors. These data were fit to a third-order polynomial weighted by errors using the IDL “poly fit” routine

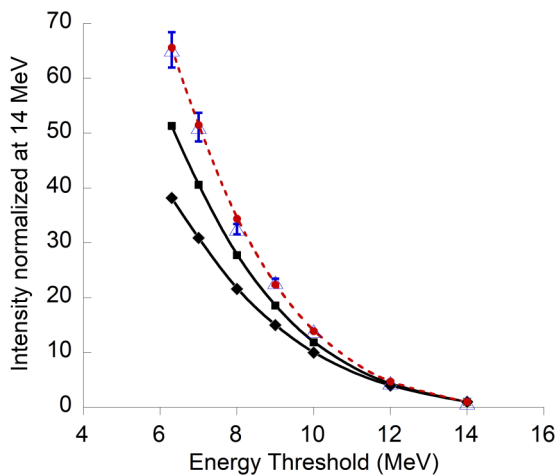


FIG. 7. Over-plot of Fig. 6 with the addition of experimental data (Δ) and the theoretical combined spectrum where the ratio has been altered to 2.1 : 1 to provide the best match to the data (\bullet).

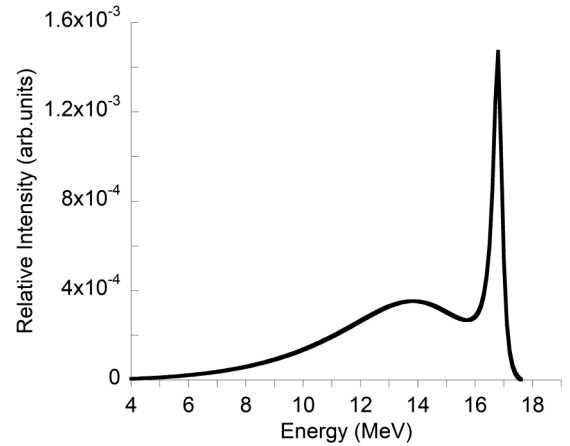


FIG. 8. The spectrum used to obtain the agreement between prediction and experiment shown in Fig. 7.

and yielded a reduced χ^2 value of 0.63. Figure 7 shows the fit to experimental data obtained and Fig. 8 shows the R -matrix spectrum used to achieve that fit. By considering errors in the fit and variations between the ITS-ACCEPT and GEANT4 codes we measured the intensity ratio $\Gamma_1 : \Gamma_0$ to be $(2.1 \pm 0.4) : 1$.

Gamma rays generated by neutron scattering from target materials, particularly from carbon in the plastic shell interfering with the measurement, were considered. However, this was discounted because the dominant γ ray from such scattering is at 4.4 MeV, which is well below the threshold energy of the GCD at maximum operating pressure (6.3 MeV). Other carbon lines above the minimum threshold are too weak to interfere with the fusion gamma signal.

IV. SUMMARY

In summary the results (Figs. 7 and 8) substantiate that the DT γ -ray spectrum is not a single line and that there exists a significant low-energy component to this DT γ -ray spectrum. The prediction of the spectral shapes of the excited and ground-state transitions for the DT reaction has been indirectly validated by the comparison to the D^3He mirror reaction and agreement with previous accelerator experiments [1]. If the assumption is made that R -matrix spectra are accurate representations for the transition to the ground and intermediate-excited states in the DT case, then the ICF data and analysis indicate an optimal ratio of the intensities of the γ -ray emissions from transitions to the intermediate-excited and the ground state $\Gamma_1 : \Gamma_0 = (2.1 \pm 0.4) : 1$. This substantiates the first spectral measurement of DT γ -ray emission to definitively identify the 5He intermediate excited-state transition in an ICF experiment.

An ICF experiment using D^3He fuel would allow a direct comparison to the results of Ref. [1]. However, the lower cross section and hence lower yields of the D^3He reaction in combination with the sensitivity of the GCD makes it difficult to extract the D^3He gamma

spectrum. Future work using a proposed γ -ray spectrometer at the NIF [23,24] may provide a direct measurement of the DT γ -ray spectrum for comparison with the inferred R -matrix solution and the measurements presented here.

ACKNOWLEDGMENTS

The authors are especially grateful to the Laser Operations team at the Laboratory for Laser Energetics, University of Rochester. UK Ministry of Defence © Crown Owned Copyright 2021/AWE.

- [1] F. E. Cecil, D. M. Cole, R. Philbin, N. Jarmie, and R. E. Brown, Reaction ${}^2\text{H}({}^3\text{He}, \gamma){}^5\text{Li}$ at center-of-mass energies between 25 and 60 keV, *Phys. Rev. C* **32**, 690 (1985).
- [2] W. Buss, W. D. Bianco, H. Waffler, and B. Ziegler, Deuteron capture in ${}^3\text{He}$, *Nucl. Phys. A* **112**, 47 (1968).
- [3] F. E. Cecil and F. J. Wilkinson, Measurement of the Ground-State Gamma-Ray Branching Ratio of the dt Reaction at Low Energies, *Phys. Rev. Lett.* **53**, 767 (1984).
- [4] J. E. Kammeraad, J. Hall, K. E. Sale, C. A. Barnes, S. E. Kellogg, and T. R. Wang, Measurement of the cross-section ratio ${}^3\text{H}(d, \gamma){}^5\text{He}$ / ${}^3\text{H}(d, \alpha)n$ at 100 keV, *Phys. Rev. C* **47**, 29 (1993).
- [5] G. L. Morgan, P. W. Lisowski, S. A. Wender, R. E. Brown, N. Jarmie, J. F. Wilkerson, and D. M. Drake, Measurement of the branching ratio ${}^3\text{H}(d, \gamma){}^3\text{H}(d, n)$, *Phys. Rev. C* **33**, 1224 (1986).
- [6] E. I. Moses, R. N. Boyd, B. A. Remington, C. J. Keane, and R. Al-Ayat, The national ignition facility: Ushering in a new age for high energy density science, *Phys. Plasmas* **16**, 041006 (2009).
- [7] Y. Kim, J. M. Mack, H. W. Herrmann, C. S. Young, G. M. Hale, S. Caldwell, N. M. Hoffman, S. C. Evans, T. J. Sedillo, A. McEvoy, J. Langenbrunner, H. H. Hsu, M. A. Huff, S. Batha, C. J. Horsfield, M. S. Rubery, W. J. Garbett, W. Stoeffl, E. Grafil, L. Bernstein *et al.*, Determination of the D-T branching ratio based on inertial confinement fusion implosions, *Phys. Rev. C* **85**, 061601(R) (2012).
- [8] Y. Kim, J. M. Mack, H. W. Herrmann, C. S. Young, G. M. Hale, S. Caldwell, N. M. Hoffman, S. C. Evans, T. J. Sedillo, A. McEvoy, J. Langenbrunner, H. H. Hsu, M. A. Huff, S. Batha, C. J. Horsfield, M. S. Rubery, W. J. Garbett, W. Stoeffl, E. Grafil, L. Bernstein *et al.*, D-T gamma-to-neutron branching ratio determined from inertial confinement fusion plasmas, *Phys. Plasmas* **19**, 056313 (2012).
- [9] N. M. Hoffman, D. C. Wilson, H. W. Herrmann, and C. S. Young, Using gamma-ray emission to measure areal density of inertial confinement fusion capsules, *Rev. Sci. Instrum.* **81**, 10D332 (2010).
- [10] G. M. Hale, Use of R -matrix theory in light element evaluations, Los Alamos National Laboratory Report LA-UR-93-102 (1993).
- [11] A. Csoto and G. M. Hale, S -matrix and R -matrix determination of the low-energy ${}^5\text{He}$ and ${}^5\text{Li}$ resonance parameters, *Phys. Rev. C* **55**, 536 (1997).
- [12] D. R. Tilley, C. M. Cheves, J. L. Godwin, G. M. Hale, H. M. Hofmann, J. H. Kelley, C. G. Sheu, and H. R. Weller, Energy levels of light nuclei $A = 5, 6, 7$, *Nucl. Phys. A* **708**, 3 (2002).
- [13] F. E. Cecil, F. J. Wilkinson, R. A. Ristinen, and R. Rieppo, Experimental determination of absolute efficiency and energy resolution for NaI(Tl) and germanium gamma ray detectors at energies from 2.6 to 16.1 MeV, *Nucl. Instrum. Methods Phys. Res., Sect. A* **234**, 479 (1985).
- [14] J. D. Lindl, *Inertial Confinement Fusion: The Quest for Ignition and Energy Gain Using Indirect Drive* (AIP Press, New York, NY, USA, 1998).
- [15] T. R. Boehly, D. L. Brown, R. S. Craxton, R. L. Keck, J. P. Knauer, J. H. Kelly, T. J. Kessler, S. A. Kumpan, S. J. Loucks, S. A. Letzring, F. J. Marshall, R. L. McCrory, S. F. Morse, W. Seka, J. M. Squires, and C. P. Verdon, Initial performance results of the OMEGA laser system, *Opt. Commun.* **133**, 495 (1997).
- [16] S. E. Caldwell and R. R. Berggren, Observation of d-t fusion gamma rays, *Rev. Sci. Instrum.* **74**, 1837 (2003).
- [17] C. J. Horsfield, M. S. Rubery, J. M. Mack, C. S. Young, H. W. Herrmann, S. E. Caldwell, S. C. Evans, T. J. Sedillo, Y. H. Kim, A. McEvoy, J. S. Milnes, J. Howorth, B. Davis, P. M. O'Gara, I. Garza, E. K. Miller, W. Stoeffl, and Z. A. Ali, Development and characterization of sub-100 ps photomultiplier tubes, *Rev. Sci. Instrum.* **81**, 10D318 (2010).
- [18] R. R. Berggren, S. E. Caldwell, J. R. Faulkner, R. A. Lerche, J. M. Mack, K. J. Moy, J. A. Oertel, and C. S. Young, Gamma-ray-based fusion burn measurements, *Rev. Sci. Instrum.* **72**, 873 (2001).
- [19] J. M. Mack, R. R. Berggren, S. E. Caldwell, C. R. Christensen, S. C. Evans, J. R. Faulkner, R. L. Griffith, G. M. Hale, R. S. King, D. K. Lassh, R. A. Lerche, J. A. Oertel, D. M. Pacheco, and C. S. Young, Remarks on detecting high-energy deuterium-tritium fusion gamma rays using a gas Cherenkov detector, *Radiat. Phys. Chem.* **75**, 551 (2006).
- [20] S. Agostinelli, J. Allison, K. Amako, J. Apostolakis, H. Araujo, P. Arce, M. Asai, D. Axen, S. Banerjee, G. Barrand, F. Behner, L. Bellagamba, J. Boudreau, L. Broglia, A. Brunengo, H. Burkhardt, S. Chauvie, J. Chuma, R. Chytrcek, G. Cooperman *et al.*, GEANT4—a simulation toolkit, *Nucl. Instrum. Methods Phys. Res., Sect. A* **506**, 250 (2003).
- [21] J. A. Halbelib, R. P. Kensek, G. D. Valdez, S. M. Seltzer, and M. J. Berger, ITS: The integrated TIGER series of electron/photon transport codes-Version 3.0, *IEEE Trans. Nucl. Sci.* **39**, 1025 (1992).
- [22] M. S. Rubery, C. J. Horsfield, H. Herrmann, Y. Kim, J. M. Mack, C. Young, S. Evans, T. Sedillo, A. McEvoy, S. E. Caldwell, E. Grafil, W. Stoeffl, and J. S. Milnes, Monte Carlo validation experiments for the gas Cherenkov detectors at the National Ignition Facility and Omega, *Rev. Sci. Instrum.* **84**, 073504 (2013).
- [23] Y. Kim, H. W. Herrmann, T. J. Hillsbeck, K. Moy, W. Stoeffl, J. M. Mack, C. S. Young, W. Wu, D. B. Barlow, J. B. Schillig, J. R. Sims, F. E. Lopez, D. Mares, J. A. Oertel, and A. C. Hayes-Sterbenz, Gamma-to-electron magnetic spectrometer (GEMS): An energy-resolved γ -ray diagnostic for the National Ignition Facility, *Rev. Sci. Instrum.* **83**, 10D311 (2012).
- [24] Y. Kim, H. W. Herrmann, H. J. Jorgenson, D. B. Barlow, C. S. Young, W. Stoeffl, D. Casey, T. Clancy, F. E. Lopez, J. A. Oertel, T. Hillsbeck, K. Moy, and S. H. Batha, Conceptual design of the gamma-to-electron magnetic spectrometer for the National Ignition Facility, *Rev. Sci. Instrum.* **85**, 11E122 (2014).